



Cite this: *Chem. Commun.*, 2023, 59, 4328

Received 26th January 2023,
Accepted 15th March 2023

DOI: 10.1039/d3cc00364g

rsc.li/chemcomm

Fluorescence-based chemical tools for monitoring ultrasound-induced hydroxyl radical production in aqueous solution and in cells[†]

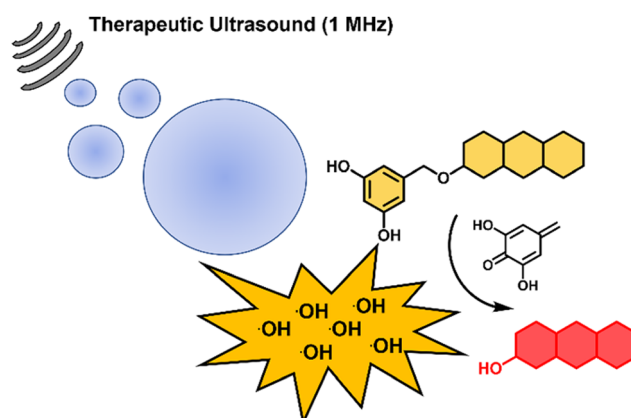
Cherie CY. Wong,^a Lu-Lu Sun,^b Meng-Jiao Liu,^c Eleanor Stride,^{id}^d
Jason L. Raymond,^{id}^a Hai-Hao Han,^{id}^{bc} James Kwan^{id}^{*a} and
Adam C. Sedgwick^{id}^{*e}

We report the synthesis of hydroxyl-radical ([•]OH) responsive fluorescent probes that utilise the 3,5-dihydroxybenzyl (DHB) functionality. 4-Methylumbelliflone-DHB (Umb-DHB) and resorufin-DHB (Res-DHB) in the presence of [•]OH radicals resulted in significant increases in their respective fluorescent emission intensities at 460 nm and 585 nm. The incubation of Res-DHB in HeLa cells followed by therapeutic ultrasound (1 MHz) resulted in a significant increase in fluorescence emission intensity thus permitting the ability to monitor ultrasound-induced [•]OH production in live cells.

The use of external stimuli to activate small molecules has shown tremendous potential in biological, biomedical and chemical research.^{1–3} Recent efforts within the chemical community have utilized the production of [•]OH radicals derived from radiolysis to activate and/or release small molecules for both imaging and therapeutic applications.^{4,5} Although a mainstay of cancer therapy, ionizing radiation suffers from several limitations, including radiation-associated toxicity and dose-limiting treatments.⁶ An emerging alternative is the use of therapeutic ultrasound, which can be used for both localised ablation⁷ and delivery/activation of anti-cancer agents.^{8,9} The ability of ultrasound to propagate through soft tissues to much greater depths than light similarly offers advantages compared with photodynamic therapy and photocaging approaches.^{10–12}

In a recent report by Peng and co-workers, ultrasound-induced cavitation effectively generated [•]OH radicals by sonolysis¹³ to activate methylene blue-based urea conjugates for both imaging and therapeutic applications.¹⁴ Inspired by this strategy, we rationalised the recently reported [•]OH radical responsive unit, 3,5-dihydroxybenzyl (DHB)⁴ may afford a general “sonocaging” unit that is selectively removed by [•]OH radicals generated from ultrasound irradiation. It is proposed [•]OH radical-mediated aromatic hydroxylation results in self-immolation releasing the active molecule (Scheme 1).

Owing to the simplicity and non-invasive nature of fluorescence probes,^{15–20} in this study, we focused on the synthesis of DHB-functionalised 4-methylumbelliflone and resorufin fluorescent probes as shown in Fig. 1 (Umb-DHB and Res-DHB). We rationalised [•]OH radicals generated by ultrasound would selectively remove the DHB unit and lead to changes in their corresponding fluorescent emissions therefore allowing us to monitor the ultrasound-induced [•]OH production in solution and in mammalian cells.^{21,22}



Scheme 1 Schematic of acoustic cavitation resulting in the [•]OH-mediated deprotection of the 3,5-dihydroxybenzyl unit and release of a highly fluorescent molecule. Grey lines depict sound waves.

^a Department of Engineering Science, Parks Road, Oxford, OX1 3PJ, UK.
E-mail: james.kwan@balliol.ox.ac.uk

^b Shandong Laboratory of Yantai Drug Discovery, Bohai Rim Advanced Research Institute for Drug Discovery, Yantai, Shandong, 264117, P. R. China.
E-mail: hanhaihao@simm.ac.cn

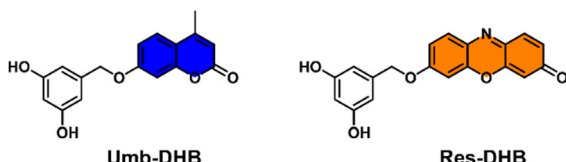
^c Molecular Imaging Center, Shanghai Institute of Materia Medica, Chinese Academy of Sciences, Shanghai, 201203, P. R. China

^d Institute of Biomedical Engineering, Department of Engineering Sciences, Old Road Campus Research Building, University of Oxford, Headington, Oxford, OX3 7DQ, UK

^e Department of Chemistry, Chemistry Research Laboratory, University of Oxford, Mansfield Road, OX1 3TA, UK. E-mail: adam.sedgwick@chem.ox.ac.uk

[†] Electronic supplementary information (ESI) available. See DOI: <https://doi.org/10.1039/d3cc00364g>



Fig. 1 Chemical structures of **Umb-DHB** and **Res-DHB**.

First, to attach the DHB unit onto each fluorophore, we synthesised a DHB-based alkylating reagent (see ESI[†] for full synthetic procedures and Schemes S1–S3). In brief, literature reported protocols were followed to isolate bis-silyl protected 3,5-dihydroxybenzyl alcohol 2.⁴ The synthetic transformation of 2 to a suitable alkylating agent proved difficult. After extensive method screening, a tosyl-based alkylating agent 3 was successfully synthesized (see ESI[†] – Scheme S1). **Umb-DHB** was obtained in 16% yield *via* refluxing 4-methylumbeliferone, 3, K₂CO₃ in THF followed by treating the crude mixture with TBAF (see ESI[†] – Scheme S2). Whereas **Res-DHB** was isolated in 27% yield by stirring resorufin, 3 and K₂CO₃ in DMF for 14 hours followed by the deprotection of the silyl ethers by treating the crude mixture with K₂CO₃ (5 eq.) and DMF (see ESI[†] – Scheme S3).²³

Next, we tested the responsiveness of **Umb-DHB** and **Res-DHB** towards [•]OH radicals generated from the Fenton reaction. These measurements were needed to confirm the [•]OH radical responsiveness of the DHB functionality.⁴ It is important to note that the Fenton reaction favours acidic pH.²⁴ However, most phenolic-based fluorophores are pH-sensitive. We therefore had to identify Fenton reaction conditions that reflected physiologically relevant pH values. Titrating Fe (ii)-EDTA to solutions of either **Umb-DHB** (5 μ M) or **Res-DHB** (5 μ M) in PBS buffer, pH = 7.40 and hydrogen peroxide (H₂O₂, 10 mM) showed an Fe (ii)-dependent (0–200 μ M, 60 min incubation) increase in fluorescence emission intensity at 460 nm and 585 nm, respectively (Fig. 2a and b and Fig. S1 and S2, ESI[†]). A colour change from orange to pink was observed for **Res-DHB**, indicative of the release of resorufin (see ESI[†] – Fig. S3). Before evaluating the response of either probe to ultrasound irradiation, we tested their reactivity to other oxidants and biologically relevant species. Acoustic inertial cavitation produces several reactive molecules,²⁵ including the reactive oxygen species (ROS): H₂O₂ and peroxy nitrite (ONOO[−]).²⁶ Surprisingly, the addition of ONOO[−] (100 μ M) led to an instant increase in the fluorescence emission intensities of both **Umb-DHB** and **Res-DHB** (Fig. 1c and d). We hypothesise this ONOO[−]-mediated response is due to the rapid decomposition of peroxy nitrous acid (ONOOH) to form [•]OH radicals.^{27,28} ONOO[−] generating the largest signal is rationalised by differences in the rate of [•]OH radical production from each source. The Fenton reaction is slow (>60 min) and suboptimal at pH = 7.4.^{24,29} This observation is supported by a similar response being seen using the traditional [•]OH radical fluorescent assay, terephthalic acid³⁰ (TA) (see ESI[†] – Fig. S4). The potential formation of ONOO[−] during sonication provides another means of deprotection for the DHB functionality.²⁶

With the responsiveness of **Umb-DHB** (5 μ M) and **Res-DHB** (5 μ M) towards [•]OH radicals identified; we turned our attention

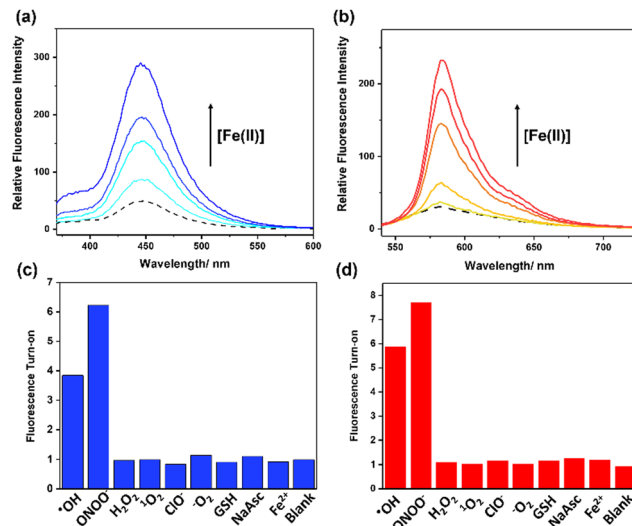


Fig. 2 (a) Fluorescent spectra of **Umb-DHB** (5 μ M) with increasing concentrations of Fe(II)-EDTA (0–200 μ M, $\lambda_{\text{ex}} = 350$ nm, 60 min incubation, Slit widths: 10 and 2.5). (b) Fluorescent spectra of **Res-DHB** (5 μ M) with increasing concentrations of Fe(II)-EDTA (0–200 μ M, $\lambda_{\text{ex}} = 500$ nm, 60 min incubation, Slit widths: ex 10 nm and em 3.5 nm). These measurements were performed in PBS buffer solution pH = 7.40 and H₂O₂, (10 mM) (c) Changes in relative fluorescence intensity of **Umb-DHB** (5 μ M) at 460 nm with other ROS and biologically relevant species (100 μ M each species) at $\lambda_{\text{ex}} = 350$ nm, Slit widths: ex 10 nm and em 2.5 nm. (d) Changes in relative fluorescence intensity of **Res-DHB** (5 μ M) at 585 nm with other ROS and biologically relevant species (100 μ M each species) at $\lambda_{\text{ex}} = 500$ nm, Slit widths: ex 10 nm and em 3.5 nm. These measurements were performed in PBS buffer solution pH = 7.40.

to monitoring changes in their respective fluorescence emissions when exposed to ultrasound (1 MHz) produced from a bespoke sonoreactor (see ESI[†] – methods). The bespoke sonoreactor was designed to create a region of high intensity ultrasound and hence acoustic cavitation in a water filled vessel. As seen in Fig. 3a and b, an increase in fluorescence emission was seen with increasing sonication time (0–6 min) at 1.2 W cm^{−2} time averaged power per unit area. The release of each fluorophore was confirmed by LC-MS analysis (see ESI[†] – Fig. S5–S8) and the TA assay confirmed the ultrasound-induced production of [•]OH radicals (see ESI[†] – Fig. S9).³⁰ It is important to note that the ultrasound parameters need further optimisation in order to fully convert each probe to the corresponding fluorophores.

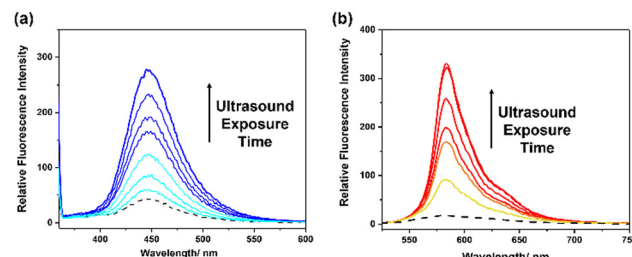


Fig. 3 (a) Fluorescent spectra of **Umb-DHB** (5 μ M) with increasing exposure time to ultrasound (1.083 MHz, 1.2 W cm^{−2}) in PBS, pH = 7.40 (b) Fluorescent spectra of **Res-DHB** (5 μ M) with increasing exposure time to ultrasound (1.083 MHz, 1.2 W cm^{−2}) in PBS, pH = 7.40.



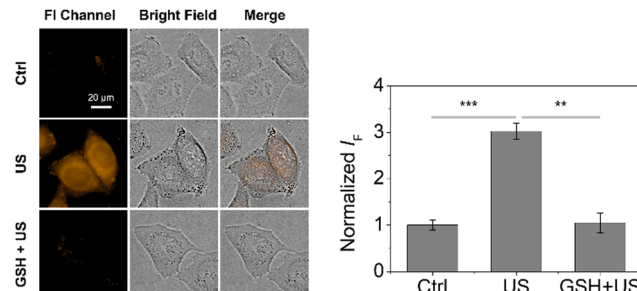


Fig. 4 Fluorescence imaging and quantification of HeLa cells incubated with **Res-DHB** (10 μ M) with and without the addition of GSH (10 mM) upon sonication. Ultrasound: 1 MHz, 1.5 $W\text{ cm}^{-2}$, 50% duty cycle, 6 ms pulse length. Time: 5 min. Mean values \pm standard deviation, $N = 3$. ** $P < 0.01$, *** $P < 0.001$.

Resorufin was chosen in this study due to its extensive use in fluorescence probe design for imaging key chemical biomarkers *in vitro* and *in vivo*.^{31,32} We hypothesized that **Res-DHB** may have the potential to image ultrasound-induced production of $\cdot\text{OH}$ radicals in live cells. However, to demonstrate the potential of this strategy in biological settings, we had to first evaluate the fluorescence response of **Res-DHB** to ultrasound generated from a clinically used commercial instrument – WED-100 (1 MHz). The fluorescence response of **Res-DHB** correlated with intensity (0, 0.5, 1.5, 2 $W\text{ cm}^{-2}$ for 5 min) and increasing duration of ultrasound irradiation (0, 5, 10, 15, 20, 25, 30 min at 1.5 $W\text{ cm}^{-2}$) (see ESI[†] – Fig. S10). The release of resorufin was confirmed by mass spectrometry (see ESI[†] – Fig. S11). In addition, we synthesised other bis-functionalised benzyl resorufin derivatives (**R1–R9**) including 3,5-dimethoxybenzyl³³-functionalised resorufin in an effort to identify additional $\cdot\text{OH}$ radical responsive units. To our surprise and despite literature precedent with ionising radiation,^{4,33} only **Res-DHB** afforded noticeable changes in fluorescence emission intensity when sonicated for 5 min and 10 min (see ESI[†] – Fig. S12). This suggests that ionizing radiation may deprotect these types of protecting groups by additional mechanisms.

With the promise shown by **Res-DHB** using WED-100, we next turned to evaluating the responsiveness of **Res-DHB** to ultrasound-induced $\cdot\text{OH}$ radical production in live cells. CCK-8 assay was first performed to evaluate the cell viability of HeLa cells when incubated with different concentrations of **Res-DHB**. Both **Res-DHB** and the parent fluorophore resorufin were found non-toxic at the relevant fluorescence imaging concentrations (0–10 μ M) and imaging timeframe (>2 h) (see ESI[†] – Fig. S13). No toxicity was seen for the duration of the ultrasound irradiation (5 min, 1.5 $W\text{ cm}^{-2}$) – see ESI[†] – Fig. S14. We next incubated **Res-DHB** (10 μ M) for 120 min followed by sonication (1.5 $W\text{ cm}^{-2}$) for 5 minutes. As seen in Fig. 4, this treatment resulted in a significant increase (3-fold) in fluorescence emission compared to the HeLa cells not exposed to ultrasound irradiation. This increase in fluorescence emission was dependent on exposure time (0–10 min) and power (0–2 $W\text{ cm}^{-2}$) (see ESI[†] – Fig. S15 and S16). In addition, pork tissue (2 cm) placed between the cells followed by ultrasound treatment (1.5 $W\text{ cm}^{-2}$, 5 min) showed

that distance did not impact the ultrasound induced fluorescence response (see ESI[†] – Fig. S17). However, due to the ROS-dependent nature of this strategy and the complexity of cellular environments, we subsequently tested the fluorescence response in the presence of the antioxidant GSH.³⁴ As seen in Fig. 4, GSH had a clear inhibitory effect on the ultrasound-induced fluorescence response (Fig. 4). This data suggests that this ultrasound-induced activation could be limited to cell types due to GSH concentrations ranging vastly in cancers.³⁵

In summary, we have synthesised two hydroxyl-radical ($\cdot\text{OH}$) responsive fluorescent probes (**Umb-DHB** and **Res-DHB**) that utilise the DHB functionality. Fluorescence changes were observed in solution and in cells when irradiated with therapeutic ultrasound frequency. However, GSH concentration was found to impact the ultrasound-induced fluorescence response in HeLa cells. These observations highlight the potential of ultrasound activation of small molecules, however further work is needed to identify the correct ultrasound parameters and cell types for this strategy to be appropriate. Further work is ongoing in our laboratories.

H.-H. H. thanks the National Natural Science Foundation of China (No. 22107029). A. C. S. would like to thank the Glasstone Research fellowship (University of Oxford) and Jesus College, Oxford for support as Junior Research Fellow. C. CY. W. thanks the Department of Engineering Science (University of Oxford) and Balliol College (University of Oxford) for their support through the DTP scholarship and the Dervouilla Scholarship, respectively.

Conflicts of interest

There are no conflicts to declare.

References

1. L. Josa-Cullere and A. Llebaria, *ChemPhotoChem*, 2021, **5**, 298–316.
2. K. S. Troelsen, E. D. D. Calder, A. Skwarska, D. Sneddon, E. M. Hammond and S. J. Conway, *ChemMedChem*, 2021, **16**, 3691–3700.
3. M. S. Baker, H. Kim, M. G. Olah, G. G. Lewis and S. T. Phillips, *Green Chem.*, 2015, **17**, 4541–4545.
4. Q. F. Fu, H. Y. Li, D. B. Duan, C. L. Wang, S. Y. Shen, H. M. Ma and Z. B. Liu, *Angew. Chem., Int. Ed.*, 2020, **59**, 21546–21552.
5. J. Geng, Y. C. A. Zhang, Q. Gao, K. Neumann, H. Dong, H. Porter, M. Potter, H. Ren, D. Argyle and M. Bradley, *Nat. Chem.*, 2021, **13**, 805–810.
6. K. Wang and J. E. Tepper, *Ca-Cancer J. Clin.*, 2021, **71**, 437–454.
7. C. A. Speed, *Rheumatology*, 2001, **40**, 1331–1336.
8. L. J. Delaney, S. Isguvan, J. R. Eisenbrey, N. J. Hickok and F. Forsberg, *Mater. Adv.*, 2022, **3**, 3023–3040.
9. T. Kondo, in *Sonochemistry and the Acoustic Bubble*, ed. F. Grieser, P.-K. Choi, N. Enomoto, H. Harada, K. Okitsu and K. Yasui, Elsevier, Amsterdam, 2015, pp. 207–230, DOI: [10.1016/B978-0-12-801530-8.00009-8](https://doi.org/10.1016/B978-0-12-801530-8.00009-8).
10. G. Gunaydin, M. E. Gedik and S. Ayan, *Front. Chem.*, 2021, **9**, DOI: [10.3389/fchem.2021.686303](https://doi.org/10.3389/fchem.2021.686303).
11. R. Weinstain, T. Slanina, D. Kand and P. Klán, *Chem. Rev.*, 2020, **120**, 13135–13272.
12. E. Beguin, S. Shrivastava, N. V. Dezhkunov, A. P. McHale, J. F. Callan and E. Stride, *ACS Appl. Mater. Interfaces*, 2019, **11**, 19913–19919.
13. M. Y. Choi, *Molecules*, 2019, **24**, 3341, DOI: [10.3390/molecules24183341](https://doi.org/10.3390/molecules24183341).

14 Y. Tong, M. Li, H. Huang, S. Long, W. Sun, J. Du, J. Fan, L. Wang, B. Liu and X. Peng, *J. Am. Chem. Soc.*, 2022, **144**, 16799–16807.

15 H. R. Bolland, E. M. Hammond and A. C. Sedgwick, *Chem. Commun.*, 2022, **58**, 10699–10702.

16 D. Wu, A. C. Sedgwick, T. Gunnlaugsson, E. U. Akkaya, J. Yoon and T. D. James, *Chem. Soc. Rev.*, 2017, **46**, 7105–7123.

17 X.-L. Hu, A. C. Sedgwick, D. N. Mangel, Y. Shang, A. Steinbrueck, K.-C. Yan, L. Zhu, D. W. Snelson, S. Sen, C. V. Chau, G. Juarez, V. M. Lynch, X.-P. He and J. L. Sessler, *J. Am. Chem. Soc.*, 2022, **144**, 7382–7390.

18 H.-H. Han, H. Tian, Y. Zang, A. C. Sedgwick, J. Li, J. L. Sessler, X.-P. He and T. D. James, *Chem. Soc. Rev.*, 2021, **50**, 9391–9429.

19 W.-T. Dou, H.-H. Han, A. C. Sedgwick, G.-B. Zhu, Y. Zang, X.-R. Yang, J. Yoon, T. D. James, J. Li and X.-P. He, *Sci. Bull.*, 2022, **67**, 853–878.

20 H.-H. Han, H.-M. Wang, P. Jangili, M. Li, L. Wu, Y. Zang, A. C. Sedgwick, J. Li, X.-P. He, T. D. James and J. S. Kim, *Chem. Soc. Rev.*, 2023, **52**, 879–920.

21 L. C. Moores, D. Kaur, M. D. Smith and J. S. Poole, *J. Org. Chem.*, 2019, **84**, 3260–3269.

22 A. R. Waggoner, Y. Abdulrahman, A. J. Iverson, E. P. Gibson, M. A. Buckles and J. S. Poole, *J. Phys. Org. Chem.*, 2021, **34**, e4278.

23 Z.-Y. Jiang and Y.-G. Wang, *Tetrahedron Lett.*, 2003, **44**, 3859–3861.

24 C. Y. Chang, Y. H. Hsieh, K. Y. Cheng, L. L. Hsieh, T. C. Cheng and K. S. Yao, *Water Sci. Technol.*, 2008, **58**, 873–879.

25 K. Peng, F. G. F. Qin, R. Jiang, W. Qu and Q. Wang, *Ultrason. Sonochem.*, 2022, **88**, 106067.

26 G. Mark, H. P. Schuchmann and C. von Sonntag, *J. Am. Chem. Soc.*, 2000, **122**, 3781–3782.

27 J. W. Coddington, J. K. Hurst and S. V. Lymar, *J. Am. Chem. Soc.*, 1999, **121**, 2438–2443.

28 J. S. Beckman, T. W. Beckman, J. Chen, P. A. Marshall and B. A. Freeman, *Proc. Natl. Acad. Sci. U. S. A.*, 1990, **87**, 1620–1624.

29 S. Goldstein and G. Merényi, *Methods Enzymol.*, 2008, **436**, 49–61.

30 J. C. Barreto, G. S. Smith, N. H. Strobel, P. A. McQuillin and T. A. Miller, *Life Sci.*, 1995, **56**, Pl89–Pl96.

31 J. W. Yoon, S. Kim, Y. Yoon and M. H. Lee, *Dyes Pigm.*, 2019, **171**, 107779.

32 L. Tian, H. Feng, Z. Dai and R. Zhang, *J. Mater. Chem. B*, 2021, **9**, 53–79.

33 J. M. Quintana, D. Arboleda, H. Hu, E. Scott, G. Luthria, S. Pai, S. Parangi, R. Weissleder and M. A. Miller, *Bioconjugate Chem.*, 2022, **33**, 1474–1484.

34 H. J. Forman, H. Zhang and A. Rinna, *Mol. Aspects Med.*, 2009, **30**, 1–12.

35 M. P. Gamesik, M. S. Kasibhatla, S. D. Teeter and O. M. Colvin, *Biomarkers*, 2012, **17**, 671–691.

